

Spin qubits in double quantum dots - entanglement versus the Kondo effect

A. Ramšak,^{1,2} J. Mravlje,² R. Žitko,² and J. Bonča^{1,2}

¹Faculty of Mathematics and Physics, University of Ljubljana, Ljubljana, Slovenia

²J. Stefan Institute, Ljubljana, Slovenia

(Dated: 26 July 2006)

We investigate the competition between pair entanglement of two spin qubits in double quantum dots attached to leads with various topologies and the separate entanglement of each spin with nearby electrodes. Universal behavior of entanglement is demonstrated in dependence on the mutual interactions between the spin qubits, the coupling to their environment, temperature and magnetic field. As a consequence of quantum phase transition an abrupt switch between fully entangled and unentangled states takes place when the dots are coupled in parallel.

PACS numbers: 03.67.Mn, 72.15.Qm, 73.63.Kv

Introduction.— After the recent discovery of quantum computing algorithms, their practical potential led to the interest in quantum entanglement spurred on by the fact that if a quantum computer were built, it would be capable of tasks impracticable in classical computing[1]. Nanostructures consisting of coupled quantum dots are candidates for required scalable solid state arrays of electron spin qubits[2, 3]. The interaction of such qubits with the environment is in general a complicated many-body process and its understanding is crucial for experimental solid state realisation of qubits in single and double quantum dots (DQD)[4]. Recent experiments on semiconductor double quantum dot devices have shown that electron occupation may be controlled down to the single-electron level by surface gates[5]. Also spin entangled states were detected[6], DQDs were used to implement two-electron spin entanglement[7], and coherent manipulation and projective readout[8] was demonstrated.

The purpose of entangled qubit pairs is to convey quantum information through a computing device[1]. The entanglement of two spin qubits may be uniquely defined through von Neuman entropy or, equivalently, concurrence[9, 10]. A pair of qubits may be realised, e.g., as two separate regions, each occupied by one electron in a state $|s\rangle_{A,B}$ of either spin, $s = \uparrow$ or \downarrow . For a system in a pure state $|\Psi_{AB}\rangle = \sum_{ss'} \alpha_{ss'} |s\rangle_A \otimes |s'\rangle_B$, the concurrence as a quantitative measure for (spin) entanglement is given by[10] $C_0 = 2|\alpha_{\uparrow\downarrow}\alpha_{\downarrow\uparrow} - \alpha_{\uparrow\uparrow}\alpha_{\downarrow\downarrow}|$. Two qubits are completely entangled, $C_0 = 1$, if they are in one of the Bell states[9], e.g., singlet $|\Psi_{AB}\rangle \propto |\uparrow\downarrow\rangle - |\downarrow\uparrow\rangle$.

The setup and main results.— We focus on entanglement between two electrons confined in two adjacent quantum dots weakly coupled by electron tunneling in a controllable manner, Fig. 1(a). The inter-dot tunneling matrix element t determines not only the tunneling rate, but also the effective magnetic superexchange interaction $J \sim 4t^2/U$, where U is the scale of Coulomb interaction between two electrons confined on the same dot. By adjusting a global back-gate voltage, exactly two electrons can be confined to the dots A-B on average.

Additional gate voltages are applied to independently control tunneling to the electrodes, t_n . Depending on the values of t_n , various topologies can be realised and even for very weak coupling, the spin of confined electrons may be

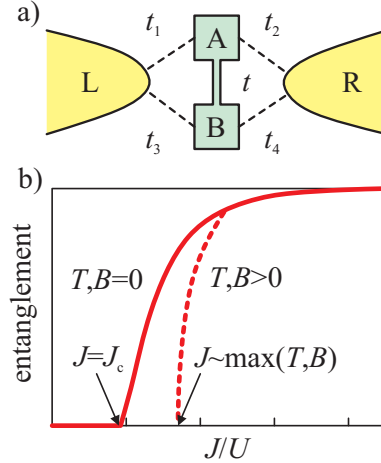


Figure 1: (color online) (a) Double quantum dot system. t and t_n are the matrix elements for tunneling between dots A and B and from the dots to the electrodes, respectively. (b) Entanglement between two spins on the quantum dots as a function of the interdot exchange coupling J : below J_c , the two spins are not entangled and the DQD is in some type of the Kondo regime. For elevated temperatures and magnetic field above J_c , the entanglement is zero if $J \lesssim \max(T, B)$.

screened due to the Kondo effect, where at temperatures below the Kondo temperature T_K a spin-singlet state is formed between a confined electron and conduction electrons close to the Fermi energy. Conductance and some other properties of such systems have already been studied, without considering, however, the analysis of the entanglement and its relationship to the many-body phenomena embodied in the Kondo effect.

Qualitatively the physics related to qubit pairs in coupled DQDs is plausible and can be summarised as:

(i) If t/U is not small the electrons tunnel between the dots and charge fluctuations introduce additional states with zero or double occupancy of individual dots[11, 12]. Due to significant local charge fluctuations this regime is not particularly appropriate for the spin-qubits manipulation.

(ii) For systems with strong electron-electron repulsion, charge fluctuations are suppressed and the states with single occupancy – the spin-qubits – dominate. Due to the effective

antiferromagnetic Heisenberg interaction the spins A and B tend to form the singlet state. The physics of such qubit pairs may be compared to the two-impurity Kondo problem studied by Jones, Varma and Wilkins two decades ago[13]. There two impurities form either two Kondo singlets with delocalised electrons or bind into a local spin-singlet state which is virtually decoupled from delocalised electrons. The crossover between the two regimes is determined by the relative values of the exchange energy J and twice the Kondo condensation energy, of order the Kondo temperature T_K .

As shown in this paper, our numerical results for representative DQD systems with different topology of possible experimental realisations reveal much more diverse physical behaviour. However, (i) in all cases the spin qubits are unentangled for J below some critical value J_c , where the actual value of J_c crucially depends on the setup topology, and (ii) at elevated temperatures $T > 0$ and external magnetic field $B \neq 0$ the entanglement is additionally suppressed and generically zero when $J \lesssim \max(J_c, T, B)$, as schematically shown in Fig. 1(b).

Quantitative results.— For simplicity we model DQD using the two-site Hubbard Hamiltonian $H = -t \sum_s (c_{As}^\dagger c_{Bs} + c_{Bs}^\dagger c_{As}) + U \sum_{i=A,B} n_{i\uparrow} n_{i\downarrow}$, where c_{is}^\dagger creates an electron with spin s in the dot $i = A$ or $i = B$ and $n_{is} = c_{is}^\dagger c_{is}$ is the number operator. The dots are coupled to the left and right noninteracting lead as shown in Fig. 1(a).

DQDs as considered here can not be described with a pure quantum state and concurrence is not directly given by C_0 . It is related to the reduced density matrix of the DQD subsystem[10, 14, 15], where for systems that are axially symmetric in spin space the concurrence may conveniently be given in the closed form[16],

$$\begin{aligned} C &= \max(0, C_{\uparrow\downarrow}, C_{\parallel}) / (P_{\uparrow\downarrow} + P_{\parallel}), \\ C_{\uparrow\downarrow} &= 2|\langle S_A^+ S_B^- \rangle| - 2\sqrt{\langle P_A^\uparrow P_B^\uparrow \rangle \langle P_A^\downarrow P_B^\downarrow \rangle}, \\ C_{\parallel} &= 2|\langle S_A^+ S_B^+ \rangle| - 2\sqrt{\langle P_A^\uparrow P_B^\uparrow \rangle \langle P_A^\downarrow P_B^\downarrow \rangle}, \end{aligned} \quad (1)$$

where $S_i^\pm = (S_i^\mp)^\dagger = c_{i\uparrow}^\dagger c_{i\downarrow}$ is the electron spin raising operator for dot $i = A$ or B and $P_i^s = n_{is}(1 - n_{i,-s})$ is the projection operator onto the subspace where dot i is occupied by one electron with spin s . $P_{\uparrow\downarrow} = \langle P_A^\uparrow P_B^\downarrow + P_A^\downarrow P_B^\uparrow \rangle$ and $P_{\parallel} = \langle P_A^\uparrow P_B^\uparrow + P_A^\downarrow P_B^\downarrow \rangle$ are probabilities for antiparallel and parallel spin alignment, respectively.

We have determined concurrence for all three possible topologically non-equivalent two terminal experimental arrangements: double quantum dots (i) coupled in series, (ii) laterally side coupled, and (iii) coupled in parallel. Concurrence was determined numerically from Eq. (1), where expectation values correspond to a many-body state with the chemical potential in the middle of the electron band, which guarantees that the dots are singly occupied, $\langle n_{A,B} \rangle = 1$. Our extensive investigation over the full parameter range for various topologies indicates that all show generic behaviour outlined in Fig. 1(b), but quantitatively can differ by many orders of

magnitude, which should be taken into consideration in experiments with such DQD. Numerical methods were based on the Gunnarsson-Schönhammer (GS) projection-operator[17, 18, 19] and numerical renormalisation group (NRG)[20, 21, 22] methods.

Serially coupled DQD.— First we consider serially coupled DQD, which models entangled pairs that may be extracted using a single-electron turnstile[23]. Here $t_{1,4} = t'$ and $t_{2,3} = 0$ with the hybridisation width of each dot $\Gamma = (t')^2/t_0$, where $4t_0$ is the bandwidth of noninteracting leads. Entanglement of a qubit pair represented with quantum dots in the contact with the leads (fermionic bath) was not quantitatively determined so far, although this system has already been extensively studied [18, 24, 25] (and references therein).

In analogy with entanglement at zero temperature studied recently in a many-body ground state[26], we consider here concurrence of DQD at fixed temperature and static magnetic field along the z -axis. Expectation values $\langle \dots \rangle$ in the concurrence formula Eq. (1) correspond to thermal equilibrium of the system, therefore $\langle S_A^+ S_B^+ \rangle = 0$ here. Qualitatively, the concurrence is significant when enhanced spin-spin correlations indicate inter-dot singlet formation. As shown in Fig. 2, the correlator $\langle \mathbf{S}_A \cdot \mathbf{S}_B \rangle$ tends to $-3/4$ for J large enough to suppress the formation of Kondo singlets, but still $J/U \ll 1$, that local charge fluctuations Δn_A^2 are sufficiently suppressed and $P_{\uparrow\downarrow} + P_{\parallel} \rightarrow 1$. Concurrence, calculated for various values of the Coulomb interaction strengths and in the absence of magnetic field is presented in Fig. 2, left bottom panel. As discussed above, C is zero for $J < J_{1c}$ due to the Kondo effect, which leads to entanglement between localised and conducting electrons[27] instead of the A-B qubit pair entanglement. In finite magnetic field irrespectively of temperature the concurrence abruptly tends to zero for $B > J$ (not shown here)[28].

In particular, the local dot-dot singlet is formed and $C \geq 0$ whenever singlet-triplet splitting $J > J_{1c} \sim 2.5T_K(\Gamma)$, where the Kondo temperature is given by the Haldane formula $T_K(\Gamma) = \sqrt{U\Gamma/2} \exp(-\pi U/8\Gamma)$. This is presented in the phase diagram in the $(U/\Gamma, J/T_K)$ plane, Fig. 3. Dashed region corresponds to the regime of zero concurrence and is delimited by the line of the critical $J = J_{1c}$ (red line). The charge fluctuations (Fig. 3, contour plot) are suppressed for sufficiently large repulsion, i.e., $U/\Gamma \gtrsim 10$. In this limit and in vanishing magnetic field, the DQD can be described in terms of the Werner states[29] and becomes similar to recently studied problem of entanglement of two Kondo spin impurities embedded in a conduction band[30]. In this case, $C_{\uparrow\downarrow} \sim 2(-\langle \mathbf{S}_A \cdot \mathbf{S}_B \rangle - \frac{1}{4}) \sim P_{\uparrow\downarrow} - 2P_{\parallel}$ for $C_{\uparrow\downarrow} \geq 0$. For large U/Γ , where the charge fluctuations vanish, the $\langle \mathbf{S}_A \cdot \mathbf{S}_B \rangle = -\frac{1}{4}$ boundary (Fig. 3, dotted line) progressively merges with the $C = 0$ line.

Side-coupled DQD.— In the side-coupled DQD configuration, $t_{1,2} = t'$, $t_{3,4} = 0$ (Fig. 2, middle), the dot A is in direct contact with the electrodes, while the dot B couples to the conduction band only indirectly through the dot A. Because the two electrodes are in contact only with dot A, is

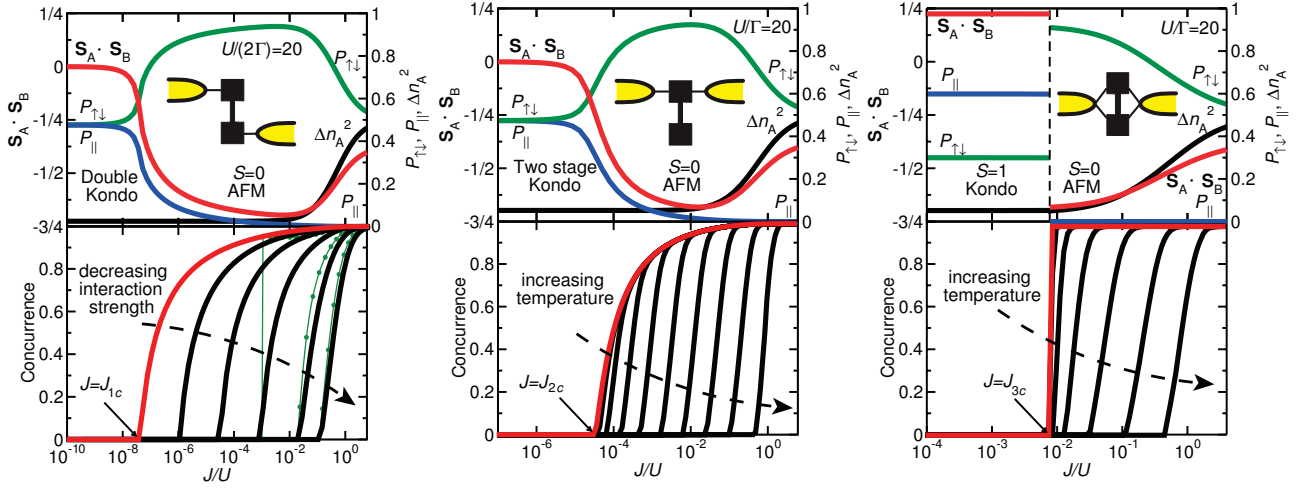


Figure 2: (color online) *Top panels:* Spin-spin correlation function $S_1 \cdot S_2$, charge fluctuations on one quantum dot, Δn_A^2 , and probabilities $P_{\uparrow\downarrow}, P_{\parallel}$ for $T \ll T_K$, $B \rightarrow 0$ and with $t' = t_0/\sqrt{20}$. *Bottom left panel:* concurrence C , corresponding to serially coupled dots, for a range of interactions $U/\Gamma = 40, 32, 24, 16, 8, 4$ and calculated with both, the NRG and the GS method (bullets), yielding the same J_{1c} , but due to the limited span of variational basis the GS method progressively overestimates C for $U/\Gamma \gtrsim 20$ regime. *Bottom right two panels:* The results for side coupled and parallel configuration obtained from the NRG method. Temperatures range from the scale of the Coulomb repulsion parameter U , $T/U = 0.4$, to temperatures below the Kondo scale T_K ; each consecutive curve corresponds to a temperature lowered by a factor 4.

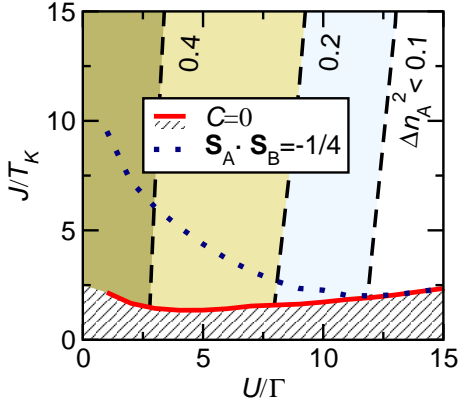


Figure 3: (color online) In the phase diagram ($U/\Gamma, J/T_K$) full line separates $C > 0$ and $C = 0$ regions (line shaded), together with dotted line indicating $\langle S_A \cdot S_B \rangle = -1/4$ ($T \rightarrow 0$ and $B = 0$). Both lines merge for $U/\Gamma \gtrsim 12$, where charge fluctuations Δn_A^2 progressively become negligible (contour plot).

$\Gamma = 2(t')^2/t_0$, i.e. twice as much as in the previous case. Since $T_K \propto \exp(-\pi U/8\Gamma)$, the Kondo temperature on dot A is strongly enhanced.

For $J > J_{2c}$, the spins bind in an antiferromagnetic singlet, as in all other cases. For $J < J_{2c}$, the system enters the ‘two stage Kondo’ regime, characterised by consecutive screening of local moments [21, 31, 32]. At the Kondo temperature $T_K^{(1)} = T_K(\Gamma)$ the spin on the dot A is screened, while the spin on the dot B is compensated at a reduced temperature

$$T_K^{(2)} = d_1 T_K^{(1)} \exp(d_2 J/T_K^{(1)}), \quad (2)$$

where $d_{1,2}$ are constants of order unity. The Kondo effect on dot A leads to the formation of a local Fermi liquid for temperatures below $T_K^{(1)}$. The quasiparticle excitations of this Fermi liquid then participate in the Kondo effect on dot B at much lower Kondo temperature $T_K^{(2)}$ [31]. Such description is valid only when the temperature scales $T_K^{(1)}$ and $T_K^{(2)}$ are widely separated. This no longer holds when J becomes comparable to $T_K^{(1)}$, see Eq. (2). The critical J_{2c} is thus still given by $J_{2c} \sim T_K^{(1)}$. The crossover is very smooth and the transition from the inter-impurity singlet phase to the Kondo phase does not exhibit any sharp features. In fact, the low temperature fixed point is the same for $J < J_{2c}$ and $J > J_{2c}$, unlike in the case of DQD in series. In the latter case, the Kondo phase and the inter-impurity singlet phase are qualitatively different and are characterised by different electron scattering phase shifts.

In the $J > J_{2c}$ singlet region, when the temperature is above J , the exchange interaction is too weak to bind the spins into a singlet and the entanglement is lost (see Fig. 2, bottom middle panel). In the $J < J_{2c}$ Kondo region, the concurrence is zero irrespective of temperature: for $T < T_K$ it is zero due to the Kondo effect, and for $T > T_K$ the spin-singlet cannot be restored, since $T > J$. Elevated temperature and magnetic field dependence is similar to the previous case of serially coupled dots [28].

Parallely coupled DQD.— In the case of parallel quantum dots ($t_n \equiv t'$ and $\Gamma = 2(t')^2/t_0$) the physics is markedly different from the case of the previous two configurations. The conduction band mediated effective Ruderman-Kittel-Kasuya-Yoshida (RKKY) interaction between the dots is, in our simplified model, ferromagnetic [22]. Here the spins or-

der ferromagnetically into a triplet state (Fig. 2, right panels) and undergo a $S = 1$ Kondo screening at low temperatures in the regime

$$J < |J_{\text{RKKY}}| \sim c \frac{64 \Gamma^2}{\pi^2 U}, \quad (3)$$

where c is a constant of order unity. This yields an uncompensated $S = 1/2$ residual spin and since half a unit of spin is quenched by the conduction band via the Kondo effect, there clearly cannot be any entanglement between the electrons on the dots. For $J > |J_{\text{RKKY}}|$, the antiferromagnetic ordering wins and, once again, the electrons form an entangled singlet state. The transition from the Kondo phase to the singlet phase is in this case a true quantum phase transition[22], and the concurrence drops abruptly from (surprisingly) $C \approx 1$, to $C = 0$ when the exchange J between the dots is decreased below some J_{3c} . Due to the sensitivity of concurrence on $J \sim J_{3c}$ can therefore parallelly coupled DQD be considered a perfect entanglement switch. Critical coupling J_{3c} is not determined by T_K , as previously, but rather by $|J_{\text{RKKY}}|$. For this reason, concurrence drops to zero at a much higher temperature (compare middle and right bottom panels in Fig. 2), and is strictly zero for $J \lesssim T$ as in previous two cases. In finite magnetic field $C = 0$ if $J \lesssim |J_{\text{RKKY}}| + B$ (not shown here)[28].

If the couplings t_n are not strictly equal, another Kondo screening stage may occur at low temperatures, in which the residual $S = 1/2$ spin is finally screened to zero[33]. In this case the quantum phase transition is replaced by a cross-over that becomes smoother as the degree of asymmetry between the couplings t_n increases (results not shown).

Conclusions.— We have found generic behaviour of spin-entanglement of an electron pair in double quantum dots. On the one hand, we have shown quantitatively that making the spin-spin exchange coupling J large by increasing tunneling t , leads to enhanced charge fluctuations, whilst on the other, a small interaction $J < J_c$ suppresses entanglement as the DQD system undergoes some form of the Kondo effect. Various regimes are explained analytically and supported with typical numerical examples. In the limiting cases we found (i) two separate Kondo effects for serially coupled DQD; (ii) two-stage Kondo effect in side-coupled DQD; and (iii) $S = 1$ Kondo effect with underscreening for parallelly coupled DQD, eventually followed by another $S = 1/2$ Kondo effect at lower temperatures. For two terminal setups, these are the only possible types of the Kondo effect; in a generic situation with arbitrary t_n , one of these possibilities must occur.

In all cases, in spite of different Kondo mechanisms, the temperature and magnetic field dependence of entanglement is proven to be determined solely by the exchange scale J and not by the much lower scale of the Kondo temperature, which explains the universal behaviour of the entanglement shown in Fig. 1(b). Critical J_c , however, will for various experimental setups vary for several orders of magnitude.

We thank I. Sega for inspiring discussions and J.H. Jefferson for valuable comments regarding the manuscript. One of the authors (A.R.) acknowledges a helpful discussion with R.H. McKenzie. We acknowledge support from the Slovenian Research Agency under contract PI-0044.

-
- [1] M. A. Nielsen and I. L. Chuang, *Quantum Computation and Quantum Information* (Cambridge University press, 2000).
 - [2] D. Loss and D. P. DiVincenzo, Phys. Rev. A **57**, 120 (1998).
 - [3] D. P. DiVincenzo, Science **270**, 255 (1995).
 - [4] W. A. Coish and D. Loss, cond-mat/0603444.
 - [5] J. M. Elzerman, R. Hanson, J. S. Greidanus, L. H. Willems van Beveren, S. D. Franceschi, L. M. K. Vandersypen, S. Tarucha, and L. P. Kouwenhoven, Phys. Rev. B **67**, 161308 (2003).
 - [6] J. C. Chen, A. M. Chang, and M. R. Melloch, Phys. Rev. Lett. **92**, 176801 (2004).
 - [7] T. Hatano, M. Stopa, and S. Tarucha, Science **309**, 268 (2005).
 - [8] J. R. Petta, A. C. Johnson, J. M. Taylor, E. A. Laird, A. Yacoby, M. D. Lukin, C. M. Marcus, M. P. Hanson, and A. C. Gossard, Science **309**, 2180 (2005).
 - [9] C. H. Bennett, H. J. Bernstein, S. Popescu, and B. Schumacher, Phys. Rev. A **53**, 2046 (1996).
 - [10] W. K. Wootters, Phys. Rev. Lett. **80**, 2245 (1998).
 - [11] J. Schliemann, D. Loss, and A. H. MacDonald, Phys. Rev. B **63**, 085311 (2001).
 - [12] P. Zanardi, Phys. Rev. A **65**, 042101 (2002).
 - [13] B. A. Jones, C. M. Varma, and J. W. Wilkins, Phys. Rev. Lett. **61**, 125 (1988).
 - [14] A. Osterloh, L. Amico, G. Falci, and R. Fazio, Nature **416**, 608 (2002).
 - [15] O. F. Syljuåsen, Phys. Rev. A **68**, 060301(R) (2003).
 - [16] A. Ramšak, I. Sega, and J.H. Jefferson, Phys. Rev. A **74**, 010304(R) (2006).
 - [17] O. Gunnarsson and K. Schönhammer, Phys. Rev. B **31**, 4815 (1985).
 - [18] J. Mravlje, A. Ramšak, and T. Rejec, Phys. Rev. B **73**, 241305(R) (2006).
 - [19] T. Rejec and A. Ramšak, Phys. Rev. B **68**, 035342 (2003).
 - [20] H. R. Krishnamurthy, J. W. Wilkins, and K. G. Wilson, Phys. Rev. B **21**, 1003 (1980).
 - [21] R. Žitko and J. Bonča, Phys. Rev. B **73**, 035332 (2006).
 - [22] R. Žitko and J. Bonča, Phys. Rev. B **74**, 045312 (2006).
 - [23] X. Hu and S. DasSarma, Phys. Rev. B **69**, 115312 (2004).
 - [24] A. Georges and Y. Meir, Phys. Rev. Lett. **82**, 3508 (1999).
 - [25] W. Izumida and O. Sakai, Phys. Rev. B **62**, 10260 (2000).
 - [26] A. N. Jordan and M. Büttiker, Phys. Rev. Lett. **92**, 247901 (2004).
 - [27] A. Rycerz, Eur. Phys. J. B **52**, 291 (2006); S. Oh and J. Kim, Phys. Rev. B **73**, 052407 (2006).
 - [28] R. Žitko, J. Bonča, and A. Ramšak, unpublished.
 - [29] R. F. Werner, Phys. Rev. A **40**, 4277 (1989).
 - [30] S. Y. Cho and R. H. McKenzie, Phys. Rev. A **73**, 012109 (2006).
 - [31] P. S. Cornaglia and D. R. Grempel, Phys. Rev. B **71**, 075305 (2005).
 - [32] M. Vojta, R. Bulla, and W. Hofstetter, Phys. Rev. B **65**, 140405(R) (2002).
 - [33] C. Jayaprakash, H. R. Krishnamurthy, and J. W. Wilkins, Phys. Rev. Lett. **47**, 737 (1981).